Chapter

An Embedded Gait Analysis System for CNS Injury Patients

Gilbert Pradel, Tong Li, Didier Pradon and Nicolas Roche

Abstract

Clinical evaluation of CNS injury patients before and after treatment is an essential step in gait rehabilitation. Medical care of gait disturbance for stroke patients is based on different treatments based on clinical and functional evaluations. Evaluation of gait aims at characterizing the motor performance to provide clinicians with information on the patient's organizational or performance status and to allow them to consider the most appropriate treatment options. A 3D instrumented gait analysis system allows quantification of several parameters at each instant of walking but does not represent gait in daily life conditions. The absence of devices usable in daily life situation constitutes a lack pointed out by clinical practitioners and is at the origin of this work. In the following are described the design and implementation of a wireless embedded system for the collection of spatiotemporal parameters of pathological gait in everyday life. Algorithms estimate joint angles, step length, and gait events and automatically partition data into gait cycles. Experiments have been carried out to accurately evaluate the joint angles, the precision of sensor synchronization, the precision of gait event detection, and the robustness in the case of pathological walk. Comparisons with references given by the 3D instrumented gait analysis system are detailed.

Keywords: CNS injury people, stroke patients, gait analysis, spatiotemporal gait parameters, gait event detection, embedded systems

1. Introduction

Stroke, caused by an effusion of the blood inside the brain tissue (hemorrhage) or by an interruption of the blood supply (ischemia), leads to motor impairments and disorders of the higher functions (e.g. negligence and anosognosia), sensorial and sensitive [1–3].

On the motor plan, the lesion of the central nervous system generates a pyramidal syndrome mainly characterized by a loss of motor selectivity, alteration of motor command, and a muscle over-activity accompanied by exaggeration of the stretch reflex commonly called spasticity. Although 50–80% of the patients recover a locomotor capacity [1, 4], they reported that, due to gait alteration, they lost a lot of autonomy in daily life activities [5–7].

Human gait is a complex phenomenon that must ensure the inter-limb coordination rotation of multiple segments in order to maintain equilibrium during motion [3]. It can be described as a series of segmental rotations of the lower limbs in order to ensure the displacement of the body. These series of cyclic movements can be split into different phases grouped together in a gait cycle. Hemiplegic patients' gait

differs from those of healthy people concerning different points like performance and organization. The main anomalies observed in this population are an alteration of spatiotemporal and kinematic parameters. Therapeutic management and prospective follow-up take into account these two points.

Medical care of gait disturbance in stroke patients use different treatments based on clinical evaluation and functional evaluation. Evaluation of the stroke patient's gait aims at characterizing the motor performance to provide clinicians with information on the patient's organizational or performance status and to allow them to consider the most appropriate treatment options.

In the same way, after applying these different therapeutic approaches, the evaluation allows the therapist to determine the effectiveness of the latter in relation to the fixed objective. Among the different methods for evaluating gait, the most commonly used to know the patient's organization during walking are the Functional Gait Assessment (FGA) and the 3D instrumented Gait Analysis (3D-GA).

There are different types of functional tests that can be used in varying scenarios to evaluate the locomotion of hemiparetic patients. Here, we just list some of the most used tests:

- The 5- or 10-m walking test: timed walk on a set distance (5 or 10 m) with spontaneous or maximum speed. With this test, the mean of speed, cadence, and step length could be determined.

- The 6-minute walk test: assesses the maximum distance walked during 6 minutes over a 30 m [8, 9] walkway to determine the average walk speed.

- The Timed Up and GO test: the patient is asked to rise from a chair, walk 3 m, turn, walk back to the chair and sit down. It can be used to assess walking speed, functional mobility, walking balance, and postural transitions.

The FGAs are performed under the situations close to those of the patient's daily life but do not provide all the parameters characterizing walking. They do not allow observing the evolution of all the parameters and also limit the number of measurable parameters; their measurement is generally not precise because it is too qualitative.

The 3D-GA provides the clinician with all the quantitative information on the state of organization of the musculoskeletal system during the execution of the locomotor task by means of the kinematic, kinetic, and spatiotemporal parameters of the gait. A 3D-GA system uses the absolute three-dimensional location of the object moving relative to a system reference also fixed. It can be typically of optoelectronic type (Motion Analysis, Vicon, Optitrack, Qualisys, Saga, Codamotion, etc.). The patient, equipped with reflective markers located on anatomical points, walks in an environment equipped with optoelectronic cameras that record the displacement of the markers, of a platform of force to detect the events of the gait cycle. A complex post processing on the recorded information extracts the locomotor parameters. This test can only be performed in a hospital environment with limitations due to the size of the environment and its duration.

The walk of the patient in the hospital environment, equipped with these reflective markers, may be not representative of his/her locomotion in everyday life: the distance is too short, the ground is horizontal without asperities, and the trajectory is very often rectilinear. When using a treadmill, the start and stop phases are delicate for the patient's balance. Also, finding a device providing information on walking is a necessity.

An embedded wearable motion analysis system uses a set of sensors worn on the body of the person to measure locomotion parameters. The system must be energy

efficient, light, and compact and must not interfere with the patient's natural locomotion so that it can be used in patients' everyday life. Information provided by the embedded system must be similar to those delivered by 3D-GA systems.

This chapter describes the wireless embedded system for acquiring the locomotor parameters of a stroke person. This system is designed to be used out of hospital environment (i.e. in the patient's daily life). This system is coupled to a gait event detection device to isolate walking cycles. The results of the experiments performed are compared to those provided by the 3D-GA in order to test the accuracy and robustness of the proposed system.

2. Changes in hemiplegic gait

2.1 Changes in spatiotemporal parameters of the gait cycle

The gait cycle, normal or pathologic, is divided into eight sub-phases: initial contact, loading response, midstance, terminal stance, pre-swing, initial swing, mid swing, and late swing [10, 11]. If the full cycle is normalized to 100%, then the stance phase (between initial contact (IC) event and final contact (FC) event) represents 60% and the swing phase 40%. This normalization makes it possible to compare the results of different studies or different populations.

The spatiotemporal parameters are often used to describe and characterize the locomotion [3, 10]. **Figure 1** illustrates the definition of the spatial parameters like step width, step length, and stride length.

The following are the temporal parameters:

- Duration of the different sub-phases, expressed in percentage
- Cadence in number of steps per minute
- Lengths of the step and the stride
- Gait speed, which is the product of the cadence per step length in m/s

If, for a healthy subject, the durations of the sub-phases in a cycle are symmetrical for the left and the right sides, it is not the case for a stroke patient. In that case, the duration of the stance phase and its percentage of the gait cycle decrease for the affected lower limb compared to the healthy subject [12–16]. Moreover, the duration of the single support phase of the paretic side is decreased compared to the healthy side. The spontaneous gait speed can be considered as a significant element that traduces patients' ability to walk [10]. Similarly, different studies [17, 18]

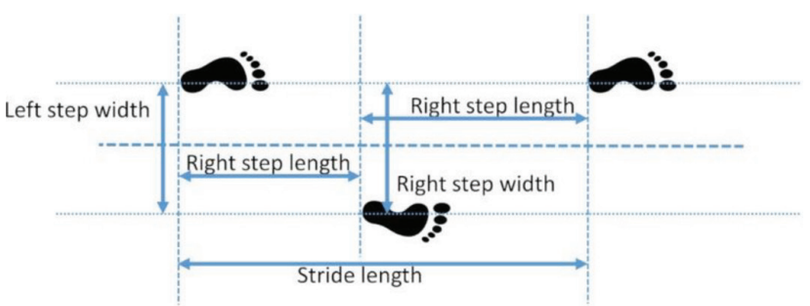

Figure 1.
Spatial parameters.

showed that the cadence of the stroke patients is decreased compared to those of the healthy subject whatever their gait speed.

2.2 Changes in joint kinematic parameters

The modifications of spatiotemporal parameters observed during gait of stroke patients are mainly caused by kinematic and kinetic alterations [19]. Global motor organization is given by the kinematic parameters, a segment rotation is characterized in function of the adjacent one, and joint angles are the main elements allowing the understanding of the gait. **Figure 2** illustrates the definition of joint angles of the lower limb.

2.2.1 Changes in movement at the hip

The joint angle of the hip is defined as the relative angle between the pelvis and the femur. The flexion/extension of the hip occurs in the sagittal plane. The flexion of the hip propels the thigh toward the anterior surface of the body. In contrast, the extension of the hip throws the thigh toward the posterior surface of the body.

For the healthy subject, at the beginning of a cycle, the hip is in flexion. During the single support phase, the hip performs an extension. At the end of propulsion, the angle of the hip reaches a maximum extension of about −10°. During the oscillating phase, the maximum value of hip flexion can reach +45°.

Usually, a stroke patient exhibits both an insufficient hip flexion and a limitation of the hip extension, [20] which contribute to the decrease of the step length and of the gait speed.

2.2.2 Changes in movement at the knee

The joint angle of the knee, defined as the relative angle between the tight and the shank, is close to +10° for the healthy subject at the beginning of a gait cycle. During the single support phase, this angle increases to a first maximum amplitude of about +20° and then decreases. At the beginning of the oscillating phase, the knee flexes quickly to prepare the oscillation of the body. We then observe a second local maximum with a value that can reach +60° followed by an extension.

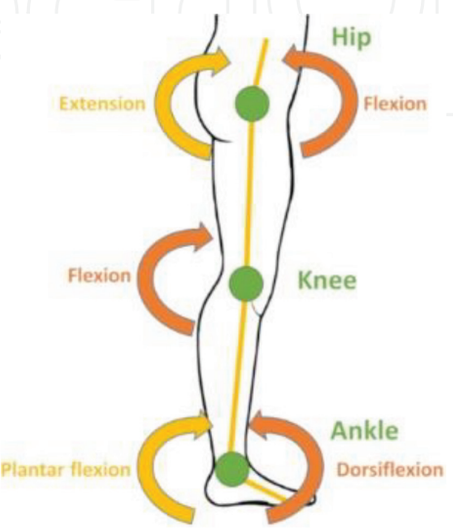

Figure 2.
Definition of the joint angles for the lower limb.

For the stroke patient, the presence of a hyper-extension at the beginning of the single support phase due to the spasticity of the triceps surae or a decrease of peak knee flexion in swing phase is called stiff knee gait mainly due to a spasticity of the rectus femoris muscle.

2.2.3 Changes in movement at the ankle

The ankle joint angle is defined as the relative angle between the shank and the foot, the foot being considered as a single rigid segment. The dorsiflexion of the ankle in the sagittal plane traduces a flexion of the foot. In contrast, plantar flexion comes from a flexion of the foot.

During the gait cycle, the evolution of ankle angle is composed by three steps:

- During the initial double contact, the heel touches the ground with the foot in neutral position (0°).
- Then, the ankle makes a plantar flexion. When the entire foot is in contact with the ground, the ankle plantar flexion is about +10°.
- After this step, the foot makes a dorsiflexion to reach a peak whose value is about +20°.
- The last step corresponds to the toe off. The ankle makes, firstly, a plantar flexion and, secondly, a dorsiflexion.

In stroke patients, a plantar flexion is often observed either during the initial double contact or during the single support phase or the swing phase. This decrease of dorsiflexion can be explained by a spasticity of the triceps surae muscle. This phenomenon is often associated with a reduction of the propulsive force and a deficit of the gait velocity [21, 22].

2.3 Discussion

During an evaluation of the therapeutic management, the following are considered:

- The relative segmental (articular kinematics) and the absolute displacements (segmental kinematics)
- The movements of the segmental and/or global center of mass by using anthropometric data, kinetics, forces, moments, and articular powers by coupling dynamometric sensors (force platform type)
- Electromyographic muscular activities

To allow appropriate management of the stoke patient, the 3D-GA system, considered de facto as the "gold standard," and the FGAs are the most used methods. However, the costs as well as the complexity of the use of optoelectronic 3D-GA systems reduce the use of this assessment of gait disturbance of patients with stroke sequelae to a limited number of laboratories/hospitals compared to the actual demand of patients.

The studies presented in the following describe the design and implementation of a wireless embedded system for collecting gait parameters of pathological gait in everyday life.

3. Recording of gait parameters by wireless wearable system

The main objective at the base of the approach is the study of the signals from the sensors during walking and the implementation of the posture estimation algorithm. This section describes the architecture of the realized prototype as well as the algorithm used to estimate the posture. The flexions and extensions of the segments estimated by the prototype are compared with the measurements from the 3D-GA system considered as a reference. The results of this comparison will be shown in the experimentation section.

3.1 System architecture

Different types of noninvasive sensors are able to measure the gait kinematics, such as magnetic sensors, goniometers, and inertial measurement units (IMU). These IMUs, consisting of sensors, measure the acceleration, the angular velocity, and the terrestrial magnetic field density around the sensor in the orthonormal coordinate system bound to the sensors. This information is used to estimate the orientation of the human body segments on which the sensors are placed. The joint angles are then calculated based on the orientations of the segments.

The IMU and compass sensor based on MEMS (Micro Electro Mechanical System) technology allow the design of miniaturized wireless sensors respecting the constraints of energy consumption, compactness, and cost. Therefore, the system uses MEMS IMU and compass sensor to capture the movement of lower limb segments.

The system comprises at least seven sensor nodes as shown in **Figure 3**. Each node is built around the System-on-Chip (SoC) Nrf51822 from Nordic Semiconductors. It offers many low-power wireless communication options, including ESB and Bluetooth Low Energy (BLE) protocols. The inertial sensor used is the MPU6050 from Invensense. This IMU integrates a 3D accelerometer and a 3D gyrometer. A 3D magnetometer is used to measure the Earth's magnetic field. Measurements carried out by the sensors are processed by the onboard SoC to estimate their orientations in real time.

A coordinator node supports the synchronization of the sensor nodes, the recording of the data coming from the sensor nodes on a SD card, and the management of the various functions of the sensor node (connection/disconnection,

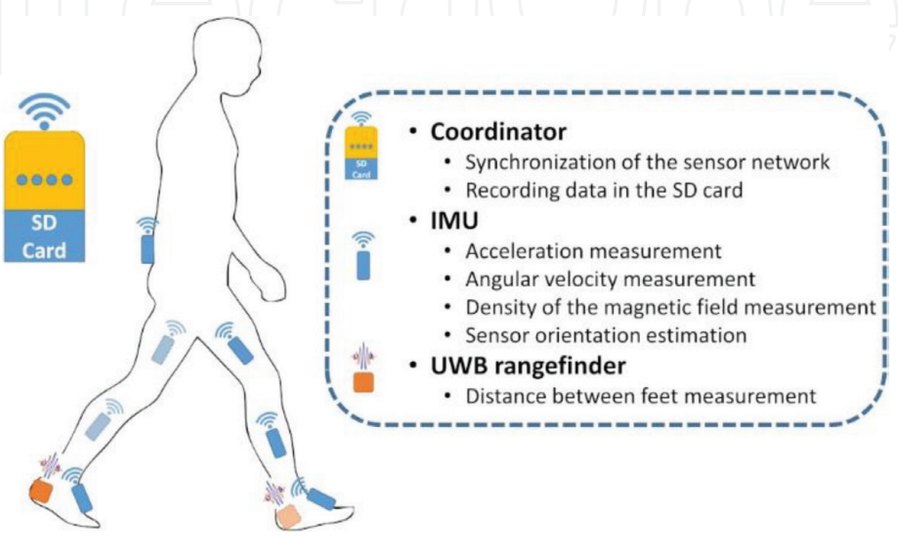

Figure 3.
System organization and sensor placement.

calibration, and power on/off). The sensor nodes wait for synchronization with the coordinator and then transmit the data to it. This wireless distributed system architecture provides great system flexibility and greatly improves its ease of use.

3.2 Constraints related to the use of a wireless device

The wireless transmission protocol, in addition to being energy efficient, must have enough bandwidth to transmit measurements in accordance with the required sampling frequency. The protocol must allow synchronization of the clocks of the various sensors to have the same time reference. Clock synchronization, imperative in our application, allows separate systems to have the smallest possible difference between their subjective times whatever the factors that can modify the time reference [23].

Candidate technologies, such as WIFI (IEEE 802.11), ZigBee (IEEE 8.2.15.4), Bluetooth classic, BLE, GSM, 3G, and LTE, have not been selected because either they do not allow a precise synchronization of the sensor nodes, or they do not provide the desired throughput or limit the number of nodes. The chosen protocol, ESB, is a proprietary low energy consumption protocol proposed by Nordic Semiconductor with a bit rate of 2 Mbps. It reaches a transmission speed of 1.2 Mbps. It supports broadcast functionality to synchronize clocks.

Without the time synchronization, the time shift between sensors may achieve 144 ms after 1 hour of measurement using a clock with accuracy equal to 20 ppm. Synchronization accuracy tests were performed. The synchronization RMSE calculated during the last minute after 1 hour of recording is equal to 18.2 μs. During the test, the maximum clock offset between two sensor nodes is 37.6 μs.

The average of the sampling period of the system, i.e. the duration between two synchronizations, equals 9.1 ms with a standard deviation of 1.1 ms. The acquisition frequency of system locomotive parameters can reach 109 Hz.

3.3 Joint angle reckoning

Each sensor node has its own reference system. It is then necessary to define a suitable coordinate system to describe the orientation of a lower limb's segment. Two coordinate systems are used in this application. One system is fixed to the earth and may be considered for the purpose of segment of human motion analysis to be an inertial coordinate system. The other coordinate system is local to the IMU and is referred to as a body coordinate system. The attitude of an object can be represented in different ways [24]. Euler angles, rotation matrix, and quaternion are the most used methods. Quaternion is difficult to understand but compared to the two other representation methods, it requires less memory and calculation capabilities. It avoids the problem of Gimbal lock that appears in Euler angle representation. The quaternion representation is used in this application. A complete description of the use of quaternions for articular angle calculation between two segments and the transformation of the local coordinate system to the terrestrial reference is described in [24, 25].

Data captured by IMU and magnetometer are processed in real time with the algorithm executed by the onboard SoC to estimate sensor attitude. This algorithm uses a numerical integration to compute the angle from the angular velocity provided by the gyrometer. This numerical integration inevitably introduces a drift in addition to the calculation approximation error. To correct this drift which accumulates over time, the information provided by the accelerometer and the magnetometer have been merged according to the onboard algorithm. The detail of this algorithm is described in [26, 27].

Finally, tests in static and dynamic conditions show that the adopted method is effective to compensate the drift of the gyrometer during walk. The quality of estimation is related to the conditions of use of the sensor (vibration, percussion, and external accelerations experienced during a long time...). Nevertheless, if the IMU works on a limit condition for a very long duration, the risk of incorrect estimated value remains present. In the case of gait in everyday life, these conditions occur periodically, but not during a long time, the precision of estimated values remains in acceptable limits.

Thanks to this system, it is possible to calculate the joint angles of the lower limb in real time and to record them in an everyday life environment.

3.4 Experiments

The experiments are carried out in a gait analysis laboratory equipped with 3D-GA system, considered as reference, to evaluate the accuracy of the proposed system. Three healthy subjects and two hemiparetic patients have been experimented with wearing markers for 3D-GA system and the wearable system. The hemiparetic patients perform 6 times a course of 8 m with self-select comfortable speed. The 3D-GA system capture area is approximately 6 m × 3 m; this limits the recording time. To evaluate the reliability of the proposed system for a longer duration, it has been decided to practice the experiments on a treadmill. To avoid the difficulties encountered by hemiparetic patients, especially when starting the carpet, only the healthy subjects have been asked to walk on the treadmill. The healthy persons have been asked to walk on the treadmill for 1 minute. The speed of the treadmill is set at 4 km/h.

Figure 4 shows the evolution of joint angles of a hemiparetic patient during walking on flat terrain (right side in blue and left side in red). The signals of both systems have a great similarity in shape. There is no time shift, and the differences between the signals from the two systems are limited.

Figure 5 illustrates the changes in joint angles in the sagittal plane of a healthy person while walking on a treadmill. The joint angles estimated by the proposed system are the continuous line signals and those measured by the 3D-GA system are in dashed line. The figure shows joint angles in a 10-second window of a 1-minute recording. As for the signals observed on the hemiplegic patient, the signals of both systems have a great similarity in shape. The two systems are well synchronized. The differences between the signals from the two systems are limited.

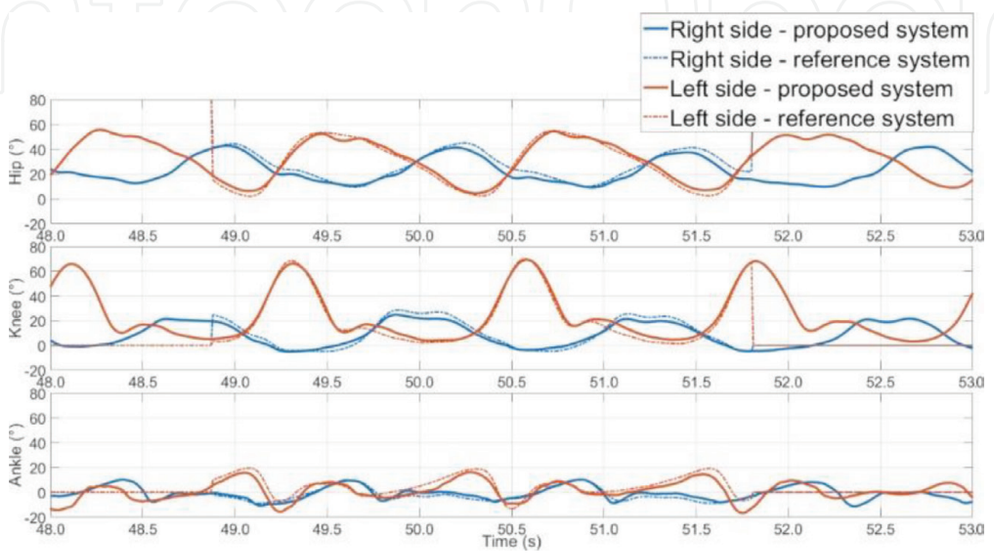

Figure 4.
Joint angles of a hemiparetic subject.

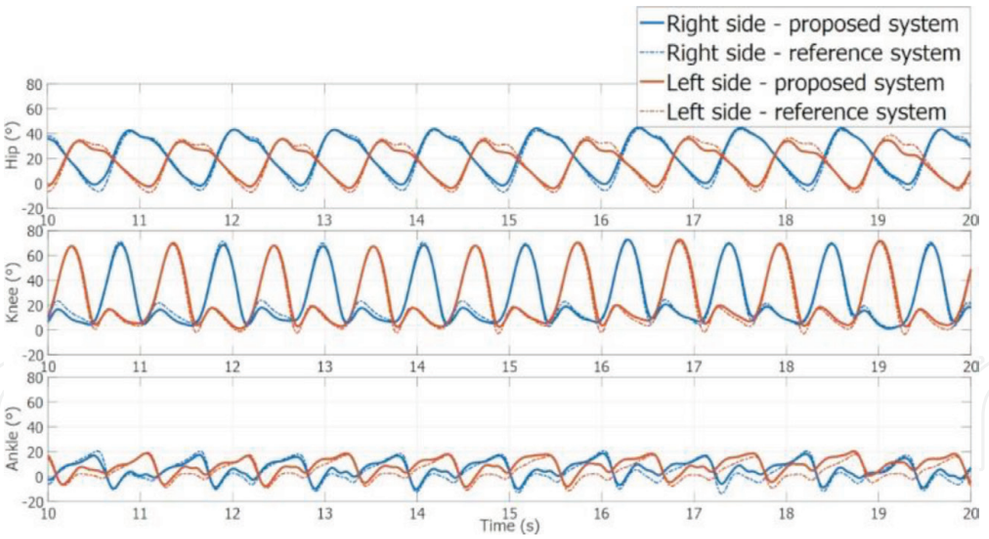

Figure 5.
Joint angles of a healthy subject during treadmill walking.

Table 1 illustrates the accuracy of the wearable system compared to the 3D-GA system. Root mean square error (RMSE) allows us to observe the difference of each sample between the two systems. The correlation coefficient (CC) allows us to evaluate the similarity of the shapes of the signals measured by the two systems. The RMSEs of joint angles estimated with respect to the reference system are between 2.4° and 4.0° for healthy persons. The CCs of healthy subjects are between 0.89 and 0.99. The signals of the hemiparetic patients have RMSEs between 3.1° and 3.6° and CCs between 0.89 and 0.99.

Figure 6 illustrates the correlation and concordance of the joint angles measured by the two systems. The coefficient of determination (r^2) equals 0.97. The lower limits of agreement (95%) equal −4.8° and the upper limits of agreement (95%) equal 7.6°.

3.5 Discussion

Comparisons between the results of the embedded system and the reference show that the joint angles measured by the embedded system have limited differences compared to the reference system. The RMSE of the proposed system is between 2.4° and 4.0°. The signal shapes of both systems have great similarities. The CC of the signals between two systems is between 0.89 and 0.99.

		Joint angle					
		Ankle		**Knee**		**Hip**	
		RMSE (°)	**CC**	**RMSE (°)**	**CC**	**RMSE (°)**	**CC**
Hemiparetic subject	1	3.6	0.90	3.3	0.98	3.5	0.98
	2	3.2	0.89	3.4	0.98	3.1	0.97
Average		3.4	0.90	3.3	0.98	3.3	0.98
Healthy subject	1	4.0	0.90	3.1	0.99	3.3	0.97
	2	3.9	0.89	3.0	0.99	2.4	0.99
	3	3.4	0.92	3.2	0.99	3.2	0.98
Average		3.8	0.90	3.1	0.99	3.0	0.98

Table 1.
Comparison between the proposed system and the 3D-GA system.

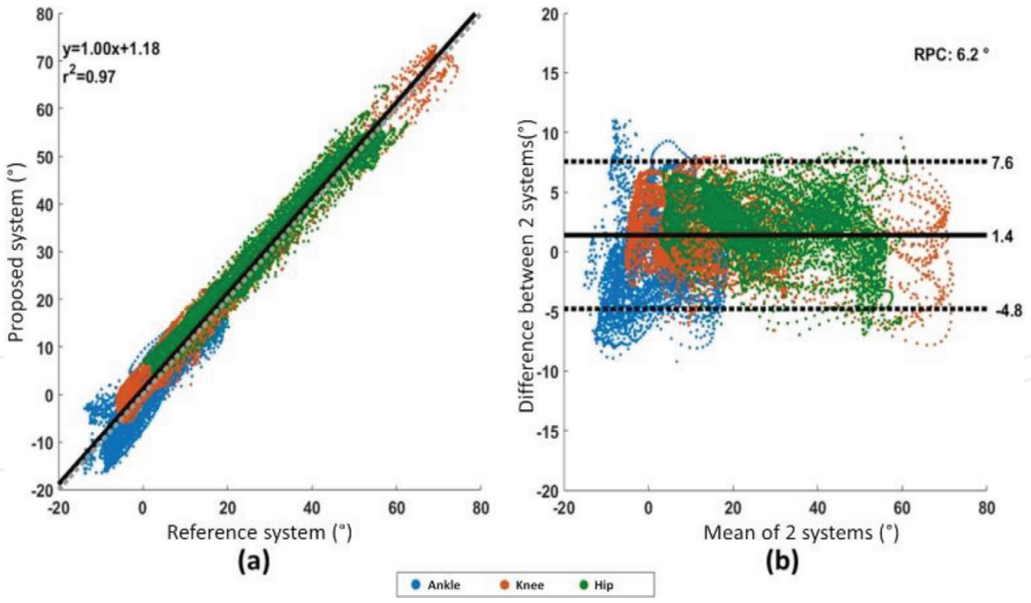

Figure 6.
Correlation (a) and Bland-Altman plot (b).

From the results of the comparison (**Table 1**), **Figures 6** and 7, the largest RMSE and the smallest CC are observed for the joint angles of the ankles. Three sources may induce these errors: percussion during walking, centripetal acceleration, and the cross-talk effect [28]. During the walk, the main percussions occur when the foot contacts the ground. Percussions influence the measurements of accelerometers and gyrometers; the filtering process used to reduce these influences does not fully eliminate them. Measurement errors can also be introduced by the cross-talk effect. During a straight walk, the ankles have more degrees of freedom than other joints. When positioning a sensor, there can be misalignments between the sensor and the segment of the human body. The consequence is that the movements in the planes other than the sagittal plane are combined in the measure. This problem can be solved by adding a calibration phase to align the sensor and human body [29]. This problem will be considered in a future study.

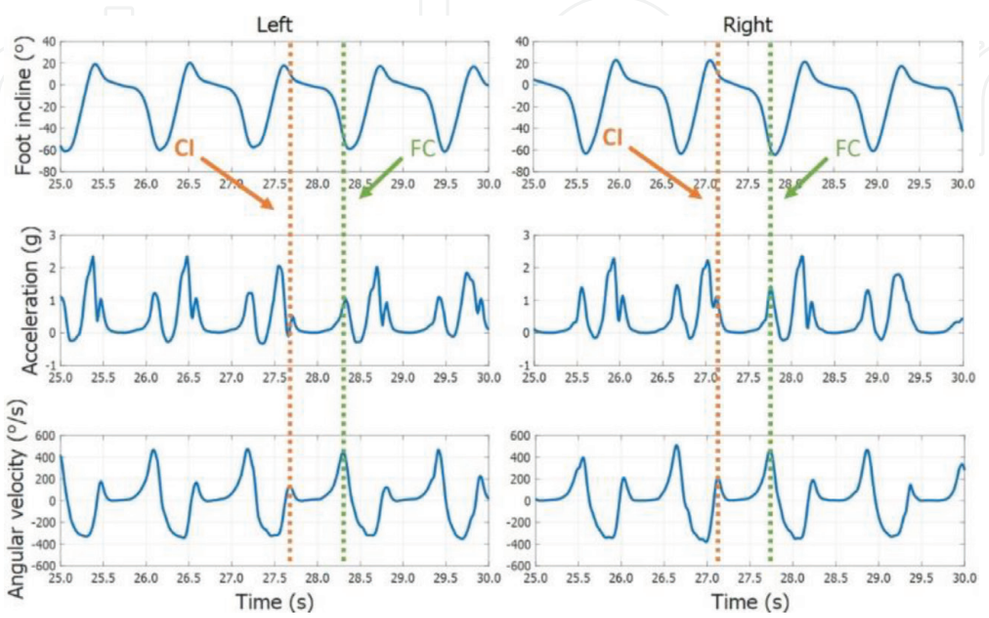

Figure 7.
IMU signals and gait events of a healthy subject.

To conclude this section, despite the lack of a precise calibration process, the embedded system provides an estimate of the joint angles close to the references, which validates both the architecture and the data processing algorithm.

Data captured by the system are organized in time series; this does not allow to analyze or compare inter or between patients. In gait analysis, locomotion data are often partitioned with gait event and normalized in gait cycle to compare with each other. The size of data captured in everyday life condition is often huge. A method to perform auto-partition is necessary.

4. Determination of gait events

Detection of gait events is a fundamental problem. All captured gait signals should be normalized in gait cycles so that they could be compared between each other. Calculations of spatiotemporal parameters are also based on the timing of gait events. So, the determination of the IC and FC event occurrences is compulsory.

In everyday life conditions, the gait event can be captured whether by measuring the ground reaction force (GRF) or by processing of the signals from IMU.

GRF-based methods use foot switches (force sensitive resistor or mechanical switch) placed under toe and heel to determine IC and FC events. Gait event detection is quite easy with these methods. Due to the GRF, the foot switch state toggles both when the foot contacts the ground (Heel-Strike, IC event) and when the foot leaves the ground (Toe-Off, FC event). These systems are considered as the Gold Standard for normal gait due to their high accuracy.

But in pathological gait, the IC event could not correspond to heel-strike and the FC event not often corresponds to toe-off as in normal gait. For example, with foot drop gait, the IC event may be the moment when the toe starts to contact the ground and FC event is the moment of toe-off. Therefore, it is difficult to place the force sensor for the pathological gait, and this limits its use [30].

Several studies propose real-time or delayed real-time motion detection systems based on the use of acceleration and angular velocity signals of human body segments provided by IMU [30–36]. All the algorithms proposed in these studies consist of a set of rules that make it possible to identify several characteristics in the different gait signals. Currently, in everyday life gait event determination systems, the accelerometer seems to be the most used sensor [37]. The data it provides are often coupled with data from the gyrometer to get more reliable results.

Figure 7 illustrates the acceleration, sagittal angular velocity, and inclination signals of both feet on a healthy subject during normal walking. The signals observed on both feet have almost the same characteristics and shapes. The local extrema of acceleration and angular velocity signals are the most commonly used characteristics for determining gait events (IC and FC) [37]. The accuracy of methods presented in different studies may achieve between 11 and 165 ms [35, 36]. Between 86 and 98% of events are correctly detected for normal gait [37].

Figure 8 shows the acceleration, angular velocity, and inclination signals of the two feet of a hemiparetic patient during a straight walk. Due to the asymmetry of the gait, the acceleration and angular velocity signals are significantly distinct between the healthy side and the paretic side. The amplitudes of the acceleration and angular velocity signals are much lower than those of a healthy person. Local maximum is strongly attenuated, especially the local maximum corresponding to the IC event in the angular velocity signal. In addition, the style of pathological walking varies greatly between stroke persons and there is a significant variability in the shape of the recordings. Given this specificity, it is difficult to use existing

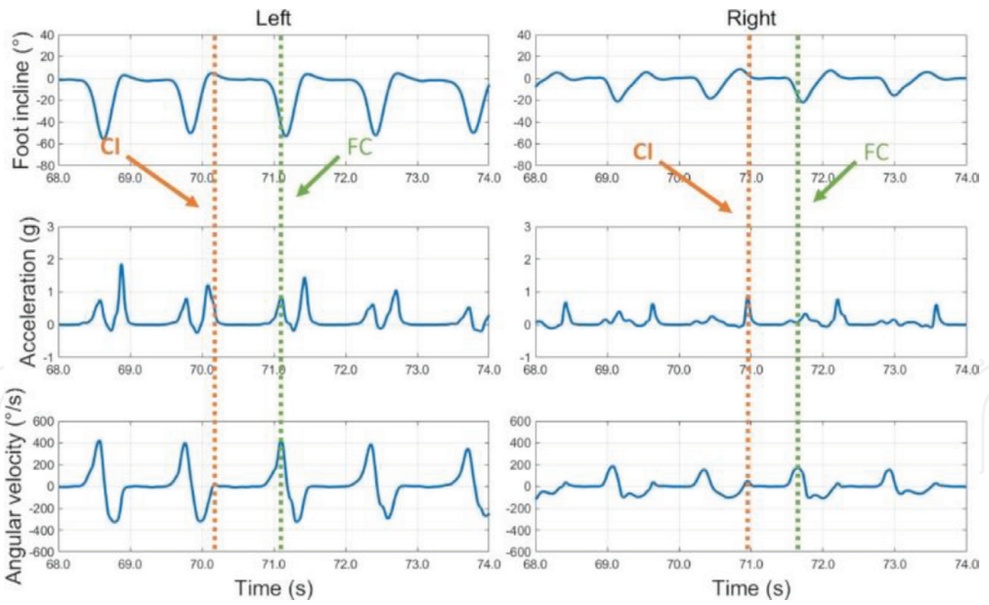

Figure 8.
IMU signals and gait events of a stroke subject.

methods to treat different types of pathological walking. An alternative method is therefore necessary to determine the gait events.

4.1 Proposed method

During walk, the distance between the two feet varies periodically. Assume, at moment t_0, the following situation: both feet are on the ground, right foot forward and left foot back. The beginning of the gait cycle of the right foot is the moment when it touches the ground. The distance between the two feet is maximum, which leads to a local maximum in the feet distance signal. During the single support phase of the right foot, the left foot being in swing phase, the distance between feet decreases until the first local minimum is reached when the left foot passes beside the right foot. This distance then increases to another local maximum when the left foot is on the ground. During the swing phase of the right foot, the second minimum appears when the right foot passes near the left foot. The gait cycle of the right foot ends with increasing distance to the third maximum when the right foot is on the ground. **Figure 9** illustrates the variation in the distance between the two feet during walking of a healthy subject and a stroke subject. Asymmetry in the length of the stroke patients justifies the larger differences in amplitude between adjacent local maximum.

Figure 10 illustrates the variation in the normalized foot distances in the gait cycle of a healthy and of a stroke person during straight walking. The two signals have similar shapes close to the letter 'w'. The signals are composed of three local maxima and two local minima. This phenomenon seeable during the gait of the healthy person is also encountered in pathological walking. The two local maxima located at the beginning and at the end of the gait cycle correspond to the IC event of the same side. The third local maximum located at around 50% of the walking cycle identifies the IC event of the opposite side. The two local minima occur as the feet pass closest to each other. It is observed that the median local maximum on the signal of the healthy people is very close to the point corresponding to 50% of walking cycle. Opposite, because of the gait asymmetry of the hemiparetic patient, the median local maximum is slightly offset from the middle point of the gait cycle.

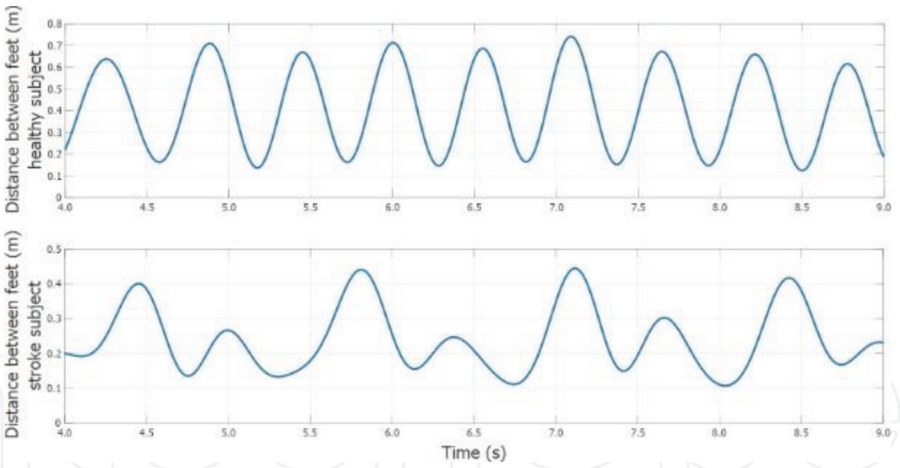

Figure 9.
Distance between feet during walk.

Compared to the acceleration and angular velocity signals, the foot distance signal is simpler to use for the recognition of gait events as the extrema are more significant. The IC event can be highlighted by searching for the local maximum of the foot distance signal.

Figure 11 shows the relationship binding the distance between the two feet and the IC event. In this figure, the blue curve is the relative distance between feet during the walk of the hemiparetic patient. This distance is captured by the 3D-GA system. The red dots correspond to the IC events determined manually by visual inspection. Green triangles are the local maximums of the distance. Local maxima are very close to the IC events determined manually. Feet distance can then be an alternative, simpler, and more robust method than existing ones.

However, local maxima only allow determining that an IC event is produced by a foot. To distinguish, the foot that produces the IC event is the one that has just finished its swing phase, because the opposite foot is in its **support** phase. The acceleration experienced by the foot that produces the IC event must be significantly greater than that of the opposite foot before the IC event. Comparing the accelerations of both feet for a time just before the IC event occurs is the way to identify the foot that produces this event.

After the IC events have been correctly determined, it is then possible to partition and normalize the recording in gait cycles. Between two IC events on the same foot, there must be a FC produced by this foot. Even if the local maxima that correspond to the IC events are attenuated and become undetectable, the local maxima

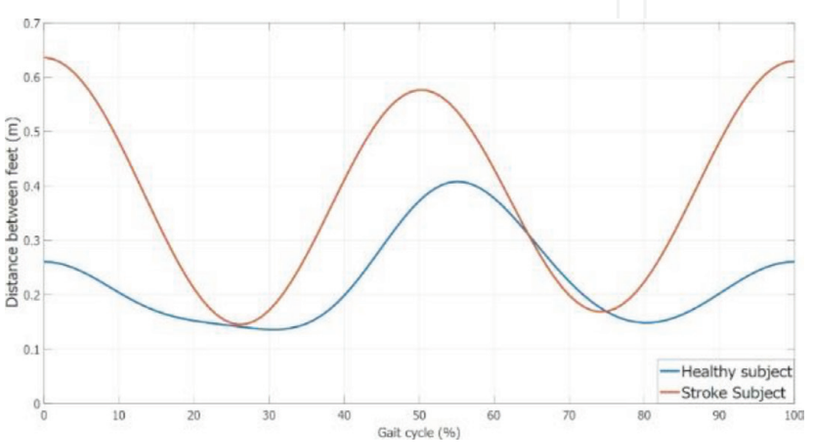

Figure 10.
Distance between feet normalized in gait cycle.

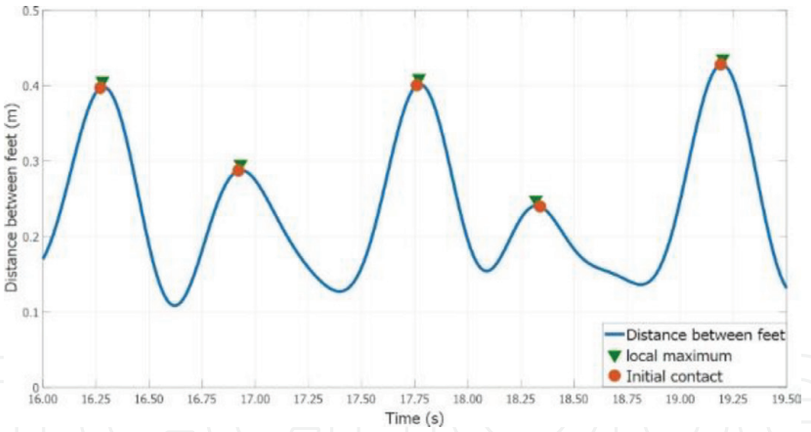

Figure 11.
Relationship between the IC event and the distance between feet.

that correspond to the FC events are still detectable. The method for determining FC using the signal from gyrometer, which is presented in different studies, remains valid [30, 33, 38, 39].

In the following, the new embedded sensor for measuring the relative distance between feet to determine the IC event is described. The data from this new sensor are coupled with data provided by the IMU to determine the FC event. The accuracy of this method is evaluated by comparing the results provided by the proposed system and those given by the 3D-GA system.

The distance between feet can be measured either by measuring the displacements of the two feet independently or by a direct measurement of the distance between the two feet.

Theoretically, the displacement of the foot can be calculated with data from the IMU attached to the foot. After estimating the attitude of the foot, a reference transformation can be made to transform the acceleration measured in the sensor coordinate system to the fixed coordinate system. By double integration on the acceleration of the foot, the three-dimensional displacement of the foot can be reckoned. But unbounded drifts will appear because of the sensor noise and the accumulation of the digital integration error.

Several studies propose different methods based on the algorithm called "zero velocity update" (ZUPT), which aim at reducing this error [40–43]. These methods are based on the detection of the period during which the foot is considered as static or quasi-static according to the information measured by the accelerometer or the gyrometer, supposing that the foot velocity is equal to zero during these periods. These methods limit the error introduced by the first integration applied to the accelerations to obtain the foot speed. However, no correction is applied to the second integration applied to the speed to calculate the displacement. This implies an accumulation of error over time on the calculation of movement of the foot. The study in [44] shows that the same displacement calculated with data from two IMUs does not give the same result. The errors depend on the style of locomotion and the gait speed as well as the type of environment in which walking is performed [45]. For this reason, none of the studies cited use the movements relative between the two feet.

In order to find a solution, a direct real-time measurement of the relative distance of the feet will be made by a wireless rangefinder that will complement the wireless system. The rangefinder measures the distance directly by measuring the time of fight (ToF) of an electromagnetic wave, thus avoiding complex calculations.

4.2 Measurement of feet distance with ultra-wideband (UWB) rangefinder

To determine gait events using foot distance signal, a pair of rangefinder modules (based on DM1000 [46]) is added to the system. The rangefinders are connected to the sensor nodes on the feet. To obtain the best performance of the distance measurement, the two rangefinders are placed at the medial side of foot, close to the heel, antennas face to face, as shown in **Figure 12**. The feet relative distance provided by the modules is coupled with the information from sensors on the feet to determine the IC and EC events and the times they occur. The rangefinders are sampled at 100 Hz. **Figure 3** illustrates the main organization and role of the elements of the final system.

4.3 Experiments

Experiments are conducted to evaluate the accuracy of the proposed system including the gait event detection and joint angle estimation. Experiments are performed in a gait analysis laboratory equipped with 3D-GA system. Totally, 11 hemiparetic patients, 4 females and 7 males 51.7 ± 18.2 years old, participated in the experiments. About, 4 healthy people, 1 female and 3 male aged 24 ± 3.1 years, participated in the experiments. The persons were equipped with both markers for 3D-GA system and proposed wearable system during experiment. All persons have been asked to walk 6 times on a straight course of 8 m with self-selected confirmable speed. The walking scenarios are captured by 3D-GA system at 100 Hz and at 70 Hz by the proposed wearable system. The embedded system's records are re-sampled at 100 Hz so that they can be compared point-to-point with those of the 3D-GA system.

Figure 13 illustrates the joint angles of a hemiparetic patient normalized in gait cycles. In this figure, the red curves represent the joint angles of the left side (healthy side) and the blue curves represent the joint angles of the right side (paretic side). The dotted curves are the angles measured by the 3D-GA system and the solid lines are the angles estimated by the proposed wearable system.

The two systems are compared by evaluating the accuracy of the gait event detection (IC and FC) and the joint angle estimation. IC and FC events' RSMEs are used to evaluate the accuracy of gait event detection, and the detection rate is calculated to describe the robustness of event detection.

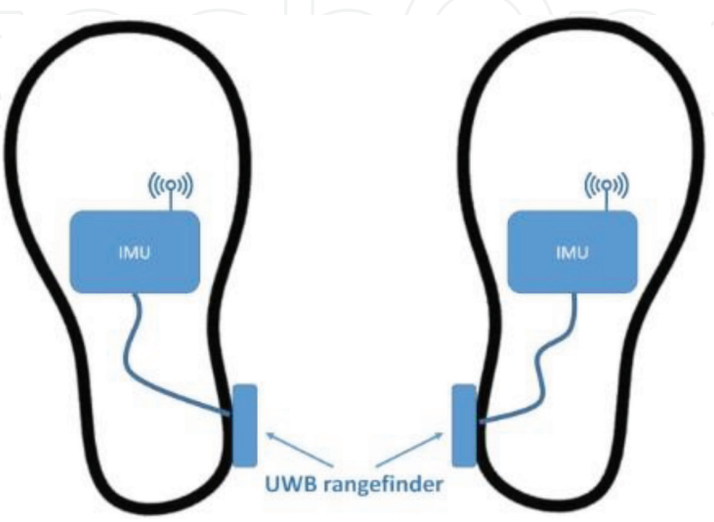

Figure 12.
Placement of rangefinder.

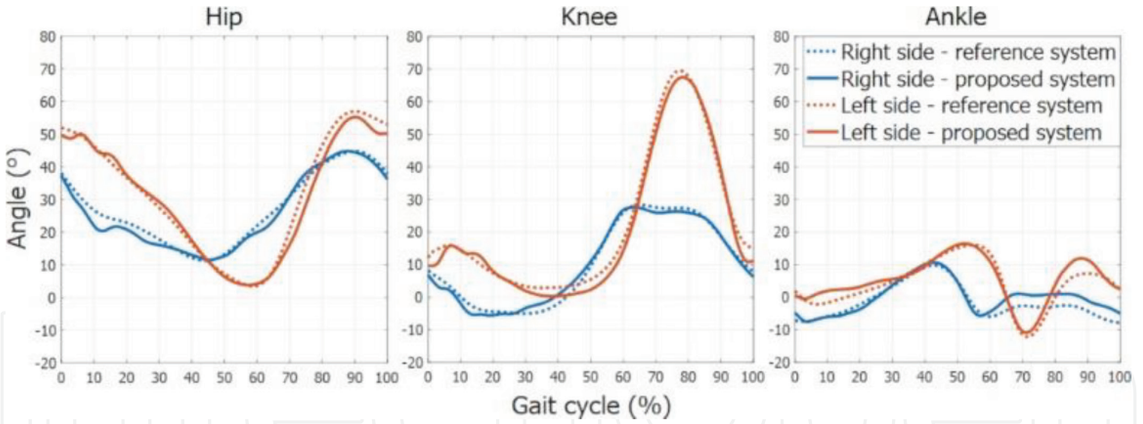

Figure 13.
Joint angles of hemiparetic subject normalized in gait cycle.

Table 2 summarizes the results of the comparison of the accuracy between the proposed system and the 3D-GA system of joint angles and gait events as well as the robustness of the gait event detection. The RMSE estimates of joint angles are between 1.3° and 3.9° for hemiparetic patients and between 1.8° and 4° for healthy subjects. The CCs for stroke subjects are between 0.9 and 0.99. For healthy persons, they are between 0.91 and 0.99. In terms of the detection of gait events, the RSMEs for IC detection are between 45 and 14 ms for hemiparetic patients and between 16 and 24 ms for healthy persons. The FC event detection has a precision between 12 and 41 ms for hemiparetic patients and between 15 and 20 ms for healthy persons. The rates of detection of CI are between 93 and 100% for hemiparetic patients and between 95 and 100% for healthy persons. The rates of detection of FC are between 92 and 100% for hemiparetic patients and between 97 and 100% for healthy people.

Figure 14 illustrates the correlation and concordance of the joint angles measured by the two systems. The coefficient of determination (r^2) equals 0.98. The lower limits of agreement (95%) equal −3.6° and the upper limits of agreement (95%) equal 5.9°.

4.4 Discussion

This chapter describes the use of a wireless rangefinder to measure the feet relative distance in order to automatically detect the gait events (IC and FC) in everyday life condition and specially to consider the differences between normal and pathological walking.

To evaluate the precision and robustness of the proposed system, experiments have been carried out on hemiparetic and healthy persons. The estimated information delivered is compared with that from the 3D-GA system. Their comparison shows that the joint angles estimated with the proposed system are quite comparable to those of the reference system. In terms of the detection of gait events, thanks to the additional information given by the rangefinders, errors are rare. The system is very robust in the case of pathological walking.

In terms of detection of gait events, the results show a precision of 27 ms for IC events of hemiparetic patients and 22 ms for FC events. More than 98% of the events are correctly detected. The results show that this method has good accuracy and is especially robust for pathological gait. However, because of the limitation of the area detectable by the 3D-GA system, the comparison can be done only between the data captured in this area. So, even if the detection rate of the events of several persons reaches 100%, one can imagine that it is possible that some events are lost during the beginning and the end of the gait.

		Joint angles						Gait events			
		Ankle		Knee		Hip		CI		CF	
		RMSE (°)	CC	RMSE (°)	CC	RMSE (°)	CC	RMSE (ms)	Rate (%)	RMSE (ms)	Rate (%)
Hemiparetic patients	1	2.1	0.95	1.9	0.99	2.3	0.98	43	100	17	100
	2	3.9	0.92	1.9	0.98	3.8	0.98	22	100	22	97
	3	2.4	0.97	2.6	0.99	3.8	0.94	25	97	17	100
	4	1.8	0.92	3.9	0.98	3.9	0.92	20	100	22	100
	5	2.6	0.94	2.9	0.99	2.6	0.98	45	98	42	98
	6	2.6	0.91	2.5	0.99	2.7	0.98	15	100	13	100
	7	3.9	0.95	3.5	0.98	3.5	0.97	35	100	41	100
	8	3.6	0.90	2.4	0.99	3	0.99	19	100	12	100
	9	2.9	0.93	3.1	0.97	3.6	0.91	28	98	15	97
	10	1.9	0.97	1.8	0.99	1.6	0.99	14	100	17	100
	11	2.5	0.95	1.3	0.99	3.6	0.99	30	93	24	92
Mean		2.75	0.94	2.53	0.99	3.13	0.97	26.91	98.73	22.00	98.55
Healthy persons	1	3.2	0.92	1.9	0.99	3.3	0.97	20	97	15	100
	2	3.1	0.94	3.7	0.98	1.2	0.99	24	98	13	97
	3	4	0.91	1.8	0.99	1.5	0.99	21	95	20	97
	4	2.7	0.93	3	0.99	2.8	0.98	16	100	12	100
Mean		3.25	0.93	2.60	0.99	2.20	0.98	20.25	97.50	15.00	98.50

Table 2.
Comparison between the proposed system and the 3D-GA system.

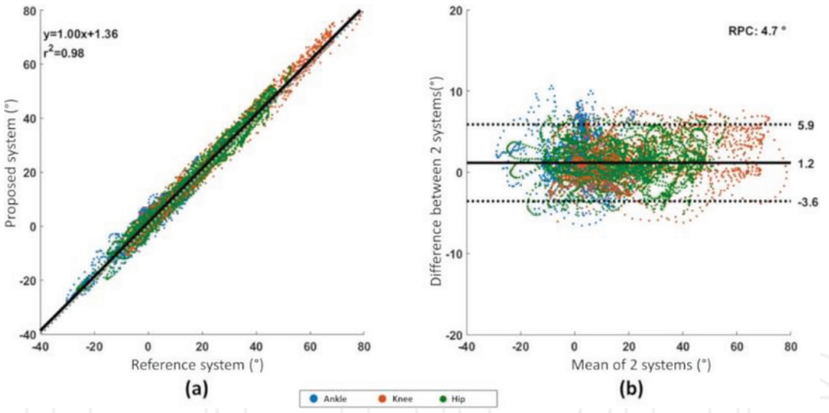

Figure 14.
Correlation (a) and Bland-Altman plot (b).

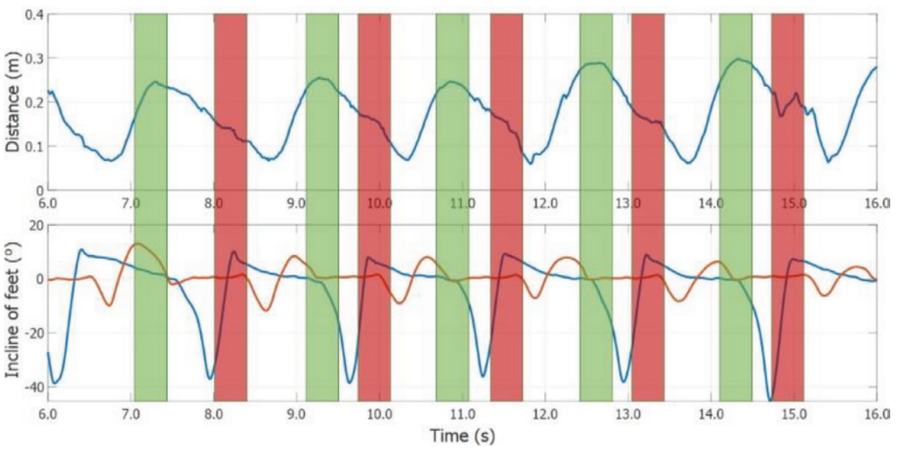

Figure 15.
CI nondetectable case.

The proposed system provides good accuracy in determining hemiparetic events but has a limitation. The method uses the relative distance between the feet as the main source of information to determine the IC event. Then, the FC is searched between two IC events. As a result, if the IC event is not correctly determined, the FC event cannot be detected. As shown in **Figure 11**, the IC events of both feet correspond to the local maximum of the relative distance signal of the feet. If the peaks corresponding to the IC are very attenuated, the risk of no longer detecting the IC event increases (**Figure 15**). This figure shows the relative distance and inclinations of the two feet. The colored areas represent the areas where the peaks on the distance signal corresponding to the IC must be observed. In green zones, significant peaks are observable; in red zones, most peaks are very attenuated or undetectable. This system cannot then be used on people that walk with a maximum distance of the feet very close to the length of the step during the double phase support. In practice, for all persons that have a minimum relative distance between feet larger than 20 cm, this system works properly.

5. Conclusion and perspectives

The chapter describes a wireless embedded system used to record information related to the gait of patients with after-effects of stroke in ecological situations.

It is based on the use of seven inertial sensors. Each sensor executes the orientation estimation algorithm. Even if each sensor uses its local clock and performs the measurement according to its own time base, their synchronization through reference broadcast time synchronization (RBTS) allows synchronization accuracy, synchronization speed, and the number of sensors to synchronize. Other constraints related to the use of the wireless link are the speed of transmission and energy consumption. To address these constraints, among wireless transmission technologies, we selected a proprietary protocol that allows the clock error between two sensors limited to a value less than 37.6 μs that does not accumulate over time. Thanks to the efficiency of this protocol, the sampling frequency to transmit the raw measurements and the orientation of the segments estimated by the sensors reaches 109 Hz.

The embedded wireless system uses a pair of range-finders to determine the gait events to split the recordings into gait cycles and calculate the temporal parameters. The method to determine the gait events, initial contact (IC) and final contact (FC), uses relative distance between feet and speed angular feet. The system also estimates the articular angles of the lower limbs. This information is the input of a piece of post-processing software that determines the temporal parameters and automatically cuts the joint angles into walking cycles. A series of experiments was conducted to evaluate the accuracy and robustness of the system. The difference between the values measured by the embedded system and the 3D-GA system shows a good robustness on the pathological path, which is quite innovative.

This development shows the evolution of our embedded gait analysis system. The final system provides the measured quantities comparable to those from a 3D-GA system. The algorithmic and material design takes into account the constraints of pathological walking and use in an ecological situation. The algorithms for segment orientation estimation and gait event detection are optimized for pathological walking. The new method we have proposed for determining the events of walking improves the robustness of event detection in the pathological case. In order for the system to be used in an ecological situation and to record the activity of the person in his daily life, the electronic design of the system is carried out in order to minimize the influence of the system on the walking of people and to have enough autonomy to record walking all day long. An effort has also been made to improve the ease of implementation and use.

In addition, it is possible to analyze the walk in more complex or functional situations. Indeed, certain clinical tests required different movements on the patient. This is the case, for example, for the TUG (Timed Up and Go). This test requires the patient to get up from a chair, walk forward 3 m, turn around a pad, walk back, and then sit down again. This test involves several motor skills. According to the chronometric performance, the risk of falling for the patient was identified for a number of values. We also looked to turn strategies in this test for stroke patients compared to healthy subjects from the quantification of the pelvis trajectory [47]. To make these comparisons, DTW (Dynamic Time Warping) methods on the trajectory of the basin on the horizontal plane were used. These methods allow identification of patients' strategies and therefore their classification as shown in [48, 49]. It is realistic to hypothesize on walking route (straight lines, stairs, up and down slopes, etc.), identification of displacement strategies from the calculation of the DTW on joint kinematics and/or segmental accelerations to follow the evolution (improvement or degradation) of the locomotor possibilities of the patient. This promising approach is the main line of our current work.

Author details

Gilbert Pradel[1*], Tong Li[1], Didier Pradon[2] and Nicolas Roche[1,2]

1 END-ICAP Lab. - UMR 1179, French National Institute for Health and Medical Research, Montigny-le-Bretonneux, France

2 Raymond Poincaré Teaching Hospital (APHP), Garches, France

*Address all correspondence to: gilbert.pradel@ens-paris-saclay.fr

References

[1] Öken Ö, Yavuzer G, Ergöçen S, Yorgancıoglu ZR, Stam HJ. Repeatability and variation of quantitative gait data in subgroups of patients with stroke. Gait & Posture. 2008;**27**(3):506-511

[2] Mazzaro N, Nielsen JF, Grey MJ, Sinkjaer T. Decreased contribution from afferent feedback to the soleus muscle during walking in patients with spastic stroke. Journal of Stroke and Cerebrovascular Diseases. 2007;**16**(4):135-144

[3] Perry J, Burnfield JM. Gait Analysis: Normal and Pathological Function. 2nd ed. Thorofare, NJ: SLACK; 2010. 551 p

[4] Williams PE, Goldspink G. Changes in sarcomere length and physiological properties in immobilized muscle. Journal of Anatomy. 1978;**127**(Pt 3):459-468

[5] Bohannon RW, Andrews AW, Smith MB. Rehabilitation goals of patients with hemiplegia. International Journal of Rehabilitation Research. 1988;**11**(2):181-184

[6] Mumma CM. Perceived losses following stroke. Rehabilitation Nursing. 2000;**25**(5):192-195

[7] Pound P, Gompertz P, Ebrahim S. A patient-centred study of the consequences of stroke. Clinical Rehabilitation. 1998;**12**(4):338-347

[8] Ng SS, Tsang WW, Cheung TH, Chung JS, To FP, Yu PC. Walkway length, but not turning direction, determines the six-minute walk test distance in individuals with stroke. Archives of Physical Medicine and Rehabilitation. 2011;**92**(5):806-811

[9] Beekman E, Mesters I, Hendriks EJM, Klaassen MPM, Gosselink R, van Schayck OCP, et al. Course length of 30 metres versus 10 metres has a significant influence on six-minute walk distance in patients with COPD: An experimental crossover study. Journal of Physiotherapy. 2013;**59**(3):169-176

[10] Kharb A, Saini V, Jain YK, Dhiman S. A review of gait cycle and its parameters. International Journal of Computational Engineering & Management. 2011;**13**:6

[11] Whittle MW. Clinical gait analysis: A review. Human Movement Science. 1996;**15**(3):369-387

[12] Brandstater ME, de Bruin H, Gowland C, Clark BM. Hemiplegic gait: Analysis of temporal variables. Archives of Physical Medicine and Rehabilitation. 1983;**64**(12):583-587

[13] Knutsson E, Richards C. Different types of disturbed motor control in gait of hemiparetic patients. Brain: A Journal of Neurology. 1979;**102**(2):405-430

[14] Olney SJ, Griffin MP, McBride ID, et al. Temporal, kinematic, and kinetic variables related to gait speed in subjects with hemiplegia: A regression approach. Physical Therapy. 1994;**74**(9):872

[15] Turnbull GI, Charteris J, Wall JC. A comparison of the range of walking speeds between normal and hemiplegic subjects. Scandinavian Journal of Rehabilitation Medicine. 1995;**27**(3):175-182

[16] Hsu A-L, Tang P-F, Jan M-H. Analysis of impairments influencing gait velocity and asymmetry of hemiplegic patients after mild to moderate stroke1. Archives of Physical Medicine and Rehabilitation. 2003;**84**(8):1185-1193

[17] Woolley SM. Characteristics of gait in hemiplegia. Topics in Stroke Rehabilitation. 2001;**7**(4):1-18

[18] Balaban B, Tok F. Gait disturbances in patients with stroke. PM&R. 2014;**6**(7):635-642

[19] Olney SJ, Richards C. Hemiparetic gait following stroke. Part I: Characteristics. Gait & Posture. 1996;**4**(2):136-148

[20] Olney SJ, Griffin MP, Monga TN, McBride ID. Work and power in gait of stroke patients. Archives of Physical Medicine and Rehabilitation. 1991;**72**(5):309-314

[21] Berger W, Horstmann G, Dietz V. Tension development and muscle activation in the leg during gait in spastic hemiparesis: Independence of muscle hypertonia and exaggerated stretch reflexes. Journal of Neurology, Neurosurgery, and Psychiatry. 1984;**47**(9):1029-1033

[22] Dietz V, Sinkjaer T. Spastic movement disorder: Impaired reflex function and altered muscle mechanics. Lancet Neurology. 2007;**6**(8):725-733

[23] Zhou H, Nicholls C, Kunz T, Schwartz H. Frequency accuracy & stability dependencies of crystal oscillators. Carlet Univ Syst Comput Eng Tech Rep SCE-08-12 [Internet]. 2008. Available from: http://kunz-pc.sce.carleton.ca/thesis/CrystalOscillators.pdf

[24] Shuster MD. Survey of attitude representations. The Journal of the Astronautical Sciences. 1993;**41**:439-517

[25] Phillips WF, Hailey CE, Gebert GA. Review of attitude representations used for aircraft kinematics. Journal of Aircraft. 2001;**38**(4):718-737

[26] Li T, Pradel G. Embedded gait parameter acquisition system for hemiplegic persons—HemiGaitEm. In: Mechatronics, Mechatronics Forum International Conference, 14. Karlstad: Karlstad University; 2014. pp. 1-8

[27] Madgwick SOH, Harrison AJL, Vaidyanathan R. Estimation of IMU and MARG orientation using a gradient descent algorithm. In: 2011 IEEE International Conference on Rehabilitation Robotics. 2011. pp. 1-7

[28] Schwartz MH, Trost JP, Wervey RA. Measurement and management of errors in quantitative gait data. Gait & Posture. 2004;**20**(2):196-203

[29] Seel T, Raisch J, Schauer T. IMU-based joint angle measurement for gait analysis. Sensors. 2014;**14**(4):6891-6909

[30] Aminian K, Najafi B, Büla C, Leyvraz P-F, Robert P. Spatio-temporal parameters of gait measured by an ambulatory system using miniature gyroscopes. Journal of Biomechanics. 2002;**35**(5):689-699

[31] Micó-Amigo ME, Kingma I, Ainsworth E, Walgaard S, Niessen M, van Lummel RC, et al. A novel accelerometry-based algorithm for the detection of step durations over short episodes of gait in healthy elderly. Journal of NeuroEngineering and Rehabilitation. 2016;**13**(1). Available from: http://jneuroengrehab.biomedcentral.com/articles/10.1186/s12984-016-0145-6

[32] Pappas IP, Popovic MR, Keller T, Dietz V, Morari M. A reliable gait phase detection system. IEEE Transactions on Neural Systems and Rehabilitation Engineering. 2001;**9**(2):113-125

[33] Pappas IPI, Keller T, Mangold S, Popovic MR, Dietz V, Morari M. A reliable gyroscope-based gait-phase detection sensor embedded in a shoe insole. IEEE Sensors Journal. 2004;**4**(2):268-274

[34] Kotiadis D, Hermens HJ, Veltink PH. Inertial gait phase detection for control of a drop foot stimulator: Inertial sensing for gait phase detection. Medical Engineering & Physics. 2010;**32**(4):287-297

[35] Mansfield A, Lyons GM. The use of accelerometry to detect heel contact events for use as a sensor in FES assisted

walking. Medical Engineering & Physics. 2003;**25**(10):879-885

[36] Trojaniello D, Cereatti A, Pelosin E, Avanzino L, Mirelman A, Hausdorff JM, et al. Estimation of step-by-step spatio-temporal parameters of normal and impaired gait using shank-mounted magneto-inertial sensors: Application to elderly, hemiparetic, parkinsonian and choreic gait. Journal of NeuroEngineering and Rehabilitation. 2014;**11**:152

[37] Rueterbories J, Spaich EG, Larsen B, Andersen OK. Methods for gait event detection and analysis in ambulatory systems. Medical Engineering & Physics. 2010;**32**(6):545-552

[38] Sabatini AM, Martelloni C, Scapellato S, Cavallo F. Assessment of walking features from foot inertial sensing. IEEE Transactions on Biomedical Engineering. 2005;**52**(3):486-494

[39] Gouwanda D, Gopalai AA. A robust real-time gait event detection using wireless gyroscope and its application on normal and altered gaits. Medical Engineering & Physics. 2015;**37**(2):219-225

[40] Jimenez AR, Seco F, Prieto JC, Guevara J. Indoor pedestrian navigation using an INS/EKF framework for yaw drift reduction and a foot-mounted IMU. In IEEE; 2010. pp. 135-143. Available from: http://ieeexplore.ieee.org/document/5649300/

[41] Ojeda L, Borenstein J. Non-GPS navigation for security personnel and first responders. Journal of Navigation. 2007;**60**(03):391-407

[42] Bebek Ö, Suster MA, Rajgopal S, Fu MJ, Huang X, Çavusoglu MC, et al. Personal navigation via high-resolution gait-corrected inertial measurement units. IEEE Transactions on Instrumentation and Measurement. 2010;**59**(11):3018-3027

[43] Wang Z, Zhao H, Qiu S, Gao Q. Stance-phase detection for ZUPT-aided foot-mounted pedestrian navigation system. IEEE/ASME Transactions on Mechatronics. 2015;**20**(6):3170-3181

[44] Nilsson J-O, Skog I, Händel P. A note on the limitations of ZUPTs and the implications on sensor error modeling. In: 2012 International Conference on Indoor Positioning and Indoor Navigation (IPIN), 13-15th November 2012. 2012. Available from: http://www.diva-portal.org/smash/record.jsf?pid=diva2:575831

[45] Skog I, Nilsson J-O, Handel P. Evaluation of zero-velocity detectors for foot-mounted inertial navigation systems. Proc IPIN [Internet]. 2010. Available from: http://ieeexplore.ieee.org/xpls/abs_all.jsp?arnumber=5646936

[46] DW1000 Radio IC [Internet]. Decawave. 2018. Available from: https://www.decawave.com/product/dw1000-radio-ic/

[47] Bonnyaud C, Roche N, Van Hamme A, Bensmail D, Pradon D. Locomotor trajectories of stroke patients during oriented gait and turning. PLoS ONE. 2016;**11**(2). Available from: https://www.ncbi.nlm.nih.gov/pmc/articles/PMC4760702/

[48] Rybarczyk Y, Deters JK, Gonzalo AA, Esparza D, Gonzalez M, Villarreal S, et al. Recognition of physiotherapeutic exercises through DTW and low-cost vision-based motion capture. In: Nunes IL, editor. Advances in Human Factors and Systems Interaction (Advances in Intelligent Systems and Computing). Springer International Publishing; 2018. pp. 348-360

[49] Rybarczyk Y, Leconte L, Medina JP. Telerehabilitation Platform for Post-Arthroplasty Recovery: A Dynamic Time Warping Approach. p. 6